Author Manuscript

Author Manuscript

Author Manuscript

Author Manuscript

HHS Public Access

Author manuscript

Pediatr Res. Author manuscript; available in PMC 2017 May 14.

Published in final edited form as:

Pediatr Res. 2017 April ; 81(4): 565–571. doi:10.1038/pr.2016.240.

Long-term Effects of Recurrent Intermittent Hypoxia and Hyperoxia on Respiratory System Mechanics in Neonatal Mice

Andrew M. Dylag[1], **Catherine A. Mayer**[1], **Thomas M. Raffay**[1], **Richard J. Martin**[1], **Anjum Jafri**[1], and **Peter M. MacFarlane**[1]

[1]Department of Pediatrics, Division of Neonatology, Rainbow Babies and Children's Hospital, Case Western Reserve University School of Medicine, Cleveland, Ohio, USA

Abstract

Background—Premature infants are at increased risk for wheezing disorders. Clinically, these neonates experience recurrent episodes of apnea and desaturation often treated by increasing the fraction of inspired oxygen (FIO_2). We developed a novel paradigm of neonatal intermittent hypoxia with subsequent hyperoxia overshoots ($CIH_{O/E}$) and hypothesized that $CIH_{O/E}$ elicits long-term changes on pulmonary mechanics in mice.

Methods—Neonatal C57BL/6 mice received $CIH_{O/E}$, which consisted of 10% O_2 (1min) followed by a transient exposure to 50% FIO_2, on 10-minute repeating cycles 24hrs/day from birth to P7. Baseline respiratory mechanics, methacholine challenge, RT-PCR for pro- and anti-oxidants, radial alveolar counts (RAC), and airway smooth muscle (ASM) actin were assessed at P21 after 2-week room air recovery. Control groups were mice exposed to normoxia (N_X), chronic intermittent hyperoxia (CIH_E), and chronic intermittent hypoxia (CIH_O).

Results—$CIH_{O/E}$ and CIH_E increased airway resistance at higher doses of methacholine and decreased baseline compliance compared to N_X mice. Lung mRNA for NOX2 was increased by $CIH_{O/E}$. RAC and ASM actin were not different between groups.

Conclusions—Neonatal intermittent hypoxia/hyperoxia exposure results in long-term changes in respiratory mechanics. We speculate that recurrent desaturation with hyperoxia overshoot may increase oxidative stress and contribute to wheezing in former preterm infants.

INTRODUCTION

Bronchopulmonary Dysplasia (BPD) is the major pulmonary morbidity of prematurity, affecting up to 10,000 US infants annually (1). Increased airway reactivity and wheezing disorders are among the most common long-term pulmonary consequences of prematurity and BPD and worsen with increasing degree of prematurity (2,3). Studies of former preterm infants demonstrate a combination of increased airway resistance, decreased lung

Users may view, print, copy, and download text and data-mine the content in such documents, for the purposes of academic research, subject always to the full Conditions of use:http://www.nature.com/authors/editorial_policies/license.html#terms

Corresponding Author: Peter M. MacFarlane, PhD, 11100 Euclid Avenue, Cleveland, Ohio 44106.

Disclosure Statement: The authors report no conflict of interest.

Category of Study: Translational

Author Manuscript Author Manuscript Author Manuscript Author Manuscript

compliance, and/or increased health care utilization (hospitalizations and asthma medications) from term corrected age through adulthood (4-8). Physicians in the Neonatal Intensive Care Unit (NICU) are challenged with maintaining adequate levels of O_2 saturation while avoiding excessive periods of hypoxia and hyperoxia. Recurrent apnea and respiratory insufficiency associated with apnea of prematurity (AOP) lead to frequent episodes of O_2 desaturation despite supplemental O_2 therapy (9). Recent studies in preterm infants using pulse oximetry have well characterized the timing and incidence of these events in the first 2 months of postnatal life (10). The incidence of desaturations (<80% saturation for 10-180 seconds) increases dramatically during the first 2 postnatal weeks followed by a steady decline thereafter with extremely preterm infants experiencing over 100 desaturation events per day (11). In the clinical setting, these events are often resolved by a transient increase in the fraction of inspired oxygen (FIO_2), most commonly titrated by the bedside nurse. A consequence of increasing FIO_2 to resolve the desaturation event, however, is an ensuing "overshoot" and a transient period of relative hyperoxia above baseline (12). Clinical studies demonstrate that the majority of desaturation events treated with O_2 result in higher O_2 saturations compared to an infant's target range (13). Furthermore, there is often a period of several minutes where the delivered FIO_2 is greater than baseline after the event resolves (13). These episodes of reoxygenation following an O_2 desaturation event may be expected to exacerbate oxidative stress, but their effects on long term airway reactivity and wheezing disorders in premature infants are unknown.

Murine lung development at birth is in the saccular stage of alveolarization, similar to the premature human lung at 24-36 weeks gestation, making it a suitable candidate to model lung disease secondary to prematurity (14). This model has been validated in numerous animal models of BPD which frequently utilize sustained and continuous hyperoxia exposure to replicate the BPD phenotype (15). Animal models of chronic intermittent hypoxia have similarly been shown to worsen allergen-induced pulmonary inflammation and have deleterious effects on respiratory function (16). Chronic intermittent hypoxia is also associated with increased levels of NOX2 and reactive oxygen species (ROS) production (17). Furthermore, re-oxygenation with 50% FIO_2 after acute hypoxia exposure resulted in a transient surge in superoxide anion formation (18). This would suggest that hypoxia, followed by re-oxygenation with hyperoxia may be a potent stimulus of ROS formation. Despite these findings, the specific patterns that predispose to later lung airway injury have not been well characterized. In this study, we developed a novel neonatal mouse model of chronic intermittent hypoxia exposure with hyperoxia overshoots to determine if they have a deleterious effect on subsequent airway hyper-reactivity and respiratory mechanics. We hypothesized that neonatal chronic intermittent hypoxia with superimposed intermittent hyperoxia causes an increase in airway responsiveness to methacholine challenge and is associated with changes in pro-oxidant enzymes.

RESULTS

Body Weight

Average body weight was not significantly different between groups at P21 (N_X: 8.9 ± 1.9g; CIH_E: 8.1 ± 1.5g; $CIH_{O/E}$: 8.4 ± 1.4g; and CIH_O: 8.4 ± 1.9g; p=0.25).

Author Manuscript Author Manuscript Author Manuscript Author Manuscript

Airway Responsiveness to Methacholine

Within each group there was a significant dose-dependent increase in Rrs (Figure 1a) and decrease in Crs (Figure 1b) when challenged with methacholine. $CIH_{O/E}$ and CIH_E groups demonstrated increased respiratory system resistance at higher methacholine doses (50-200 mg/mL) compared to animals raised in room air (Figure 1a; $p<0.05$). Airway reactivity, defined as the difference between maximal contraction at the highest dose of methacholine and baseline, did not increase in the $CIH_{O/E}$ or CIH_E groups compared to N_X ($p=0.15$ and $p=0.53$ respectively). There was a consistent decrease in specific respiratory system compliance at all methacholine doses among the $CIH_{O/E}$ and CIH_E groups compared to normoxia (Figure 1b; $p<0.05$). There were no differences in resistance or compliance responses observed in the CIH_O group compared to room air controls.

Baseline Respiratory Mechanics

Baseline respiratory mechanics at P21 are shown in Figure 2. No differences in Rrs were observed between groups (Figure 2a) at baseline. Baseline sCrs was decreased and specific elastance (sH) increased in the $CIH_{O/E}$ and CIH_E groups compared to room air controls (both $p<0.05$; Figure 2b and 2c). Similarly, specific tissue damping (sG) was increased in the $CIH_{O/E}$ and CIH_E groups compared to room air controls ($p<0.05$, Figure 2d). The $CIH_{O/E}$ group demonstrated a further increase in sG compared to the CIH_E subjects ($p<0.05$, Figure 2d). No significant baseline differences were seen in the CIH_O group compared to room air controls.

Real Time PCR

In an effort to describe changes in prooxidants and antioxidants gene expression, real time PCR of lung homogenates was performed at P21 for various superoxide dismutases (SOD) and NADPH oxidases (NOX). The antioxidants SOD1, SOD2, and SOD3 and their relative fold-change from normoxia are shown (Figure 3a). SOD1 and SOD3 were decreased in CIH_E animals compared to normoxia but unchanged among other groups. SOD2 was unchanged in all groups. The prooxidants NOX1, NOX2, as well as the transcription factor and antioxidant-regulating protein nuclear factor (erythroid-derived-2)-like2 (NRF2) were also evaluated (Figure 3b). NOX1 was decreased in CIH_O compared to all other groups ($p<0.05$). NOX2 was increased in $CIH_{O/E}$ compared to all other groups ($p<0.05$). NRF2 was decreased in CIH_O compared to $CIH_{O/E}$.

Immunohistochemistry

To assess long-term effects of intermittent hypoxia and hyperoxia on alveolarization, we quantified radial alveolar counts (RAC) at P21 (Figure 4). There were no significant differences in RAC between groups. There were also no differences in the amount of airway α-smooth muscle actin between treatment groups. Representative images and staining for α-smooth muscle actin are demonstrated in Figure 5.

DISCUSSION

Prematurity is an independent risk factor for wheezing disorders among extremely and moderately preterm infants, attributed to structural lung immaturity, pulmonary surfactant

Author Manuscript Author Manuscript Author Manuscript Author Manuscript

deficiency, mechanical ventilation, and supplemental oxygen therapy (19). Furthermore, emerging evidence implicates even late preterm birth as a risk factor for impaired respiratory function attributable to differences in lung and chest wall compliance, airway tethering, and susceptibility to postnatal infections such as RSV (20). Among infants born preterm, small airway obstruction is evident with increased odds of childhood asthma and decreased forced expiratory volume (FEV_1) among infants with and without BPD (21,22). We pursued this study to determine if a mouse model of FIO_2 fluctuations, and delivery of specific patterns of oxygen exposure, contribute to pulmonary morbidity by altering respiratory mechanics, lung architecture, airway smooth muscle, and changes in prooxidant and antioxidant signaling.

In these experiments, $CIH_{O/E}$ increased airway resistance at higher methacholine doses, decreased compliance, increased elastance, and increased tissue damping in pulmonary function testing. Specific tissue damping (sG) characterizes energy dissipation in the lung and markedly increases when there are regional differences in lung ventilation (23). sG increased in $CIH_{O/E}$ compared to CIH_E suggesting that hypoxia immediately followed by hyperoxia may have some synergistic negative effect on regional respiratory mechanics. Chronic intermittent hypoxia alone had no effect on pulmonary mechanics, lung architecture, or airway smooth muscle compared to N_X controls. We did not, however, observe any corresponding changes in radial alveolar counts, airway smooth muscle hypertrophy, and mRNA expression for antioxidant and prooxidant markers except NOX2 in our $CIH_{O/E}$ treated mice. Animals exposed to CIH_E had changes almost identical to $CIH_{O/E}$ with the exception that increased NOX2 mRNA was unique to the latter group. Although these data demonstrate complex changes in lung mRNA for various pro- and anti-oxidant enzymes, the most significant observation was the increased Rrs to methacholine in the $CIH_{O/E}$ group was associated with an increase in mRNA for the pro-oxidant NOX2. Taken together, these findings suggest that minute-to-minute swings in FIO_2 above and below 21% are relevant stimuli that contribute to altered pulmonary mechanics.

The nature of intermittent hypoxia and hyperoxia events in preterm infants changes with advancing postnatal age in both timing and frequency (11). Altering these patterns places different stressors on the developing airway, potentially altering signaling pathways and disrupting lung development. Our study utilized a pattern of exposure with FIO_2 cycling between 10% and 50% in 10-minute intervals for 24hrs/day, differentiating this exposure paradigm from other conventional exposures of sustained continuous hyperoxia that have shown airway hyperreactivity, airway smooth muscle hypertrophy, and decreased bronchiolar-alveolar attachments (24,25). In addition, our model addresses the intermittent hypoxia/hyperoxia fluctuations that take place in neonatal intensive care units on the order of minutes, not hours and mimics the frequency of events (up to 100/day) documented in the NICU (11). We demonstrated deleterious effects on pulmonary function with an average FIO_2, calculated as the "area under the curve", of 30-32% in the $CIH_{O/E}$ group. These physiologic changes persist at P21, roughly correlating to the pulmonary stage in development for a toddler-aged child (14), a common point where respiratory morbidity is described from chronic lung disease due to prematurity (26). Chronic intermittent hypoxia in the absence of hyperoxia overshoot did not induce long term airway morbidity. Therefore, our characterization of at-risk patterns of intermittent hypoxia and hyperoxia may aid in

Author Manuscript Author Manuscript Author Manuscript Author Manuscript

guiding bedside management of labile preterm infants experiencing frequent apnea and desaturations to reduce hyperoxia overshoots and potentially their long-term risk of pulmonary morbidity.

Studies with different timing, frequency, and severity of intermittent hypoxia/hyperoxia compared to $CIH_{O/E}$ have observed dysfunction in angiogenic and alveolar signaling pathways. One mouse model with single, 2-hour cycles of hypoxia (12%) with hyperoxia (50%) for 7 days demonstrated downregulation of HIF-1α and VEGF, implicating altered angiogenesis and thus impaired alveolar development (27). A different paradigm of clustered intermittent hypoxia superimposed on sustained hyperoxia showed alterations in VEGF levels normalized by treatment with a superoxide dismutase mimetic, further implicating altered angiogenesis as a factor (28). It is clear that the amount, severity, timing, and pattern of these swings in oxygen exposure can have wide-ranging effects on several signaling pathways, making it an intriguing area for further study.

The mechanism by which intermittent hypoxia with hyperoxia contributes to deleterious lung function is still not well established. In contrast to previously published studies of intermittent hypoxia/hyperoxia at one week (27), alveolarization was not affected in any study group following room air recovery at P21. We proceeded to investigate changes in signaling pathways that might be implicated in functional changes in the lung. RT-PCR for both prooxidant and antioxidant markers demonstrated increased NOX2 in only the $CIH_{O/E}$ group. NOX2 was the first protein in the family of NADPH oxidase proteins to be discovered and is present in many different cell types with highest expression in phagocytes (29). It produces superoxide, peroxynitrites, and other reactive oxygen species that are involved in host defense (29). Counts for alveolar macrophages (30) were not different between the $CIH_{O/E}$ group and other groups (data not shown), suggesting the increase in NOX2 signaling is independent of the presence of inflammatory cells in the lung parenchyma. Further investigation is needed to investigate what role NOX2 is playing in this $CIH_{O/E}$ paradigm and how it interacts with other physiologic stressors.

We have evaluated changes in both airway smooth muscle and lung parenchyma as both may contribute to increased airway reactivity. The absence of airway smooth muscle hypertrophy is consistent with no change in baseline Rrs and decreased compliance might be associated with decreased alveolarization although we did not detect changes in alveolar counts. Therefore, we speculate that the pattern of intermittent exposures is having an effect on lung function that may not be anatomically detectable at this time point. These findings contrast with other models of sustained hyperoxia demonstrating increased airway smooth muscle hypertrophy with 40% sustained FIO_2 (25) underscoring the importance of studying fluctuations in inspired FIO_2 as they relate to pulmonary function and airway reactivity.

In conclusion, the $CIH_{O/E}$ paradigm of intermittent hypoxia with hyperoxia overshoots for 7 days has long-term deleterious effects on lung function at P21 after 2-week recovery in room air but no detectable effect on alveolarization or smooth muscle hypertrophy. This study, like others underscores the negative effect specific patterns of oxygen exposure can have on lung development and lung function. Piecing together the cumulative dose of oxygen with the pattern in which it is delivered may provide valuable insight into how we respond to these

Author Manuscript Author Manuscript Author Manuscript Author Manuscript

events at the bedside. Increased oxidative stress may be implicated, however, the intermittent nature of these exposures may elicit a different signature of oxygen toxicity compared to models of sustained hyperoxia. These experiments are a first step in characterizing one pattern of oxygen exposure that may be implicated in long-term respiratory morbidity in preterm infants.

METHODS

Animals and Exposures

Animal protocols were approved by the Institutional Animal Care and Use Committee at Case Western Reserve University. Timed pregnant C57BL/6 female mice (Jackson Laboratories, Bar Harbor, ME) were purchased and housed in an AAALAC accredited animal facility on 12- hour light-dark cycles with ad libitum standard food and water. Newborn mouse pups were pooled within 24 hours of birth and randomly redistributed into treatment groups. Each litter and the nursing dam was placed in a modified exposure chamber designed to permit rapid exchange of chamber gas composition according to the desired exposure paradigm. Gas flow into the chamber was modified using individual mass flow controllers (SDPROC, AALBORG Instruments & Controls, Inc., Orangeburg, New York), programmed with a command module and corresponding software. Each flow control was independently controlled to allow airflow of gases (air, nitrogen or oxygen) into the chamber to achieve the desired exposure paradigm. An O_2 sensor was placed into the exposure chamber to continuously record achieved FIO_2. A schematic of the experimental setup is shown in Figure 6.

To simulate a desaturation with hyperoxia overshoot, one group of mice were exposed to repeating cycles of hypoxia (10% O_2) immediately followed by rebound hyperoxia (50% O_2). After the chamber reached 50% O_2, room air (21% oxygen) was purged into the chamber allowing gradual return of chamber conditions to normoxia within 5 minutes (Figure 6). This exposure was repeated at 10 minute intervals, 24hrs/day for 7 days starting at P0. This treatment group that received intermittent hypoxia and hyperoxia overshoot was designated $CIH_{O/E}$. Additional groups of mice were used to assess the separate effects of chronic intermittent hypoxia (CIH_O) or hyperoxia (CIH_E). All groups were compared to control mice raised in room air for the entire exposure period. After 7 days of respective exposures, animals were returned to room air until respiratory function testing or tissue harvesting at P21.

Respiratory Mechanics

Respiratory function testing was performed at P21 for all groups (N=7-11 per group). Each animal was placed under general anesthesia (intraperitoneal ketamine 200mg/kg and xylazine 20mg/kg), tracheostomized via a 19-gauge blunt tip cannula, and placed on a commercially available small mammal ventilator (flexiVent, SCIREQ, Montreal, Canada). Each subject was then paralyzed (pancuronium bromide 10mg/kg) and mechanically ventilated with a tidal volume of 10ml/kg, 150 breaths/min, PEEP of 3cm H_2O, and FIO_2 of 50%. Animals equilibrated for five minutes on the ventilator, then two recruitment breaths of sustained inspiration up to a pressure of 30 cm H_2O for 3 seconds were administered

Author Manuscript Author Manuscript Author Manuscript Author Manuscript

followed by measurement of baseline respiratory mechanics. A dose-response curve was generated by administering aerosolized (Aeroneb, SCIREQ) methacholine (Sigma Aldrich, St. Louis, MO) for 10 seconds at increasing doses (saline control, 12.5, 25, 50, 100, and 200mg/ml). Respiratory System Resistance (R_{rs}) and Specific Respiratory System Compliance (sC_{rs}) were calculated by the ventilator software (Flexiware Version 7.2 Service Pack 2 Build 728, SCIREQ, Montreal, Canada) using a 1.2 second, 2.5 Hz single-frequency forced oscillation maneuver (31). Specific Tissue Damping (sG) and Specific Elastance (sH) were calculated using a low-frequency forced oscillation technique imparting a quasi-sinusoidal maneuver containing a wide range of frequencies. Input impedance was then analyzed through the previously described Constant Phase Model(23). Specific values for respiratory function parameters were determined by dividing the result by the inspiratory capacity of each animal at baseline.

Real Time PCR

RNA was extracted from snap-frozen lungs of 21 day old mice (N=7-16 per group) using TriZol reagent (Life Technologies, Carlsbad, CA) and quantified by Nanodrop spectroscopy (Thermo Scientific, Waltham, MA). cDNA was generated from one microgram of RNA by reverse transcription using qScript cDNA synthesis kit (Quanta Biosciences, Gaithersburg, MD). Real-time quantitative PCR was performed on a StepOne PCR system (Applied Biosystems, Foster City, CA) using TaqMan probes (Life Technologies) for SOD1 (Mm01344233_g1), SOD2 (Mm01313000_m1), SOD3 (Mm01213380_s1), NOX1 (Mm00549170_m1), NOX2 (Mm01287743_m1), NRF2 (Mm00801891_m1) compared to GAPDH (#4351309) with PerfeCTa qPCR FastMix, UNG, ROX (Quanta Biosciences, Beverly, MA). Fold-changes are reported utilizing 2^-ddCT method and StepOne software v2.3 (Applied Biosystems).

Histology and Morphometric Analysis

Animals (N=7-12 per group) were sacrificed using anesthetic overdose of ketamine/xylazine and lungs inflated with 4% paraformaldehyde at 25cm H_2O pressure on postnatal day 21. Paraffin-embedded sections (5μm) were prepared and stained with hematoxylin-eosin. Randomly chosen hematoxylin-eosin areas were photographed with 10X magnification from 7-10 animals per group. All of the morphometric and image analysis measurements were performed by a blinded investigator. The extent of alveolarization was determined by the radial alveolar count (RAC) method as previously described (32). Six terminal bronchioles per pup were analyzed for radial alveolar count, determined by counting the number of alveolar septa transected by a perpendicular line drawn from the terminal bronchiole to the nearest connective tissue septum.

Immunofluorescence and Analysis for Airway Smooth Muscle Actin

The trachea was cannulated and the lungs (N=8-10 per group) were inflation fixed (25 cmH_2O) for 10 min with 10% neutral-buffered formalin. The left lung was removed, prepared for immuno-staining, and post fixed for 2 days at 4°C. The fixed lung was embedded in paraffin and sectioned (5μm). Sections were de-paraffinized using xylene and then dehydrated in graded alcohol. Deparaffinized tissue sections were pretreated for antigen retrieval, and incubated with a monoclonal antibody against mouse anti α-smooth muscle

Author Manuscript Author Manuscript Author Manuscript Author Manuscript

actin (α-ASM; 1:400 dilution, Sigma-Aldrich, St. Louis, MO) overnight at 4°C. Immune complexes were captured with FITC-conjugated donkey anti-mouse (1:500, Alexa Fluor-488, Invitrogen, Carlsbad, CA). Appropriate negative controls were run by omitting the primary antibody to confirm nonspecific staining, which was not observed. Immunostained sections were cover slipped with Vectashield mounting medium (Vector Laboratories, Burlingame, CA) and visualized with a fluorescence microscope. Images of the immunostained sections were captured with a Rolera XR CCD camera (Q-Imaging, Surrey, Canada) mounted on a microscope (Leica Microsystems, Wetzlar, Germany). Five random images at 20X magnifications were captured from five to seven animals per group by using digital image analysis software with settings for color and size identification (*Image j*, NIH, Bathesda, MD). The area of airways and the green fluorescent areas α-ASM from five airways per animal were measured using the circular method (33). The amount of α-ASM area was expressed as α-ASM staining divided by airway basement membrane perimeter (P_{bm}).

Statistical Analysis

Data are expressed as mean ± standard error of the mean with exception of animal weights (mean ± SD). Respiratory mechanics at baseline and for each dose of methacholine exposure were performed using two-way ANOVA with repeated measures. Analysis of mRNA expression was performed with a 1-way ANOVA on the ΔCT. Radial alveolar counts and alpha smooth muscle were performed with 1-way ANOVA. Statistical significance was defined as $p < 0.05$.

Acknowledgments

Statement of Financial Support: This work was supported by the American Academy of Pediatrics Marshal Klaus Perinatal Research Award (Elk Grove Village, IL) and an endowment from the Rainbow Babies and Children's Foundation Fellowship Research Award Program (Cleveland, OH). Additional support provided by the National Institutes of Health T32-HD060537 training grant (Bethesda, MD). Dr. Dylag is the recipient of the National Institutes of Health Loan Repayment Program award (Bethesda, MD).

REFERENCES

1. Jobe AH, Bancalari E. Bronchopulmonary dysplasia. Am J Respir Crit Care Med. 2001; 163:1723–9. [PubMed: 11401896]
2. Baraldi E, Carraro S, Filippone M. Bronchopulmonary dysplasia: definitions and long-term respiratory outcome. Early Hum Dev. 2009; 85:S1–3.
3. Ehrenkranz RA, Walsh MC, Vohr BR, et al. Validation of the National Institutes of Health consensus definition of bronchopulmonary dysplasia. Pediatrics. 2005; 116:1353–60. [PubMed: 16322158]
4. Hjalmarson O, Sandberg K. Abnormal lung function in healthy preterm infants. Am J Respir Crit Care Med. 2002; 165:83–7. [PubMed: 11779735]
5. Pramana IA, Latzin P, Schlapbach LJ, et al. Respiratory symptoms in preterm infants: burden of disease in the first year of life. Eur J Med Res. 2011; 16:223–30. [PubMed: 21719396]
6. Hennessy EM, Bracewell MA, Wood N, et al. Respiratory health in pre-school and school age children following extremely preterm birth. Arch Dis Child. 2008; 93:1037–43. [PubMed: 18562451]
7. Fawke J, Lum S, Kirkby J, et al. Lung function and respiratory symptoms at 11 years in children born extremely preterm: the EPICure study. Am J Respir Crit Care Med. 2010; 182:237–45. [PubMed: 20378729]

Author Manuscript Author Manuscript Author Manuscript Author Manuscript

8. Northway WH Jr. Moss RB, Carlisle KB, et al. Late pulmonary sequelae of bronchopulmonary dysplasia. N Engl J Med. 1990; 323:1793–9. [PubMed: 2247118]
9. Abu-Shaweesh JM, Martin RJ. Neonatal apnea: what's new? Pediatr Pulmonol. 2008; 43:937–44. [PubMed: 18780339]
10. Martin RJ, Wang K, Koroglu O, Di Fiore J, Kc P. Intermittent hypoxic episodes in preterm infants: do they matter? Neonatology. 2011; 100:303–10. [PubMed: 21986336]
11. Di Fiore JM, Bloom JN, Orge F, et al. A higher incidence of intermittent hypoxemic episodes is associated with severe retinopathy of prematurity. J Pediatr. 2010; 157:69–73. [PubMed: 20304417]
12. Baerts W, Lemmers PM, van Bel F. Cerebral oxygenation and oxygen extraction in the preterm infant during desaturation: effects of increasing FiO(2) to assist recovery. Neonatology. 2011; 99:65–72. [PubMed: 20639679]
13. van Zanten HA, Tan RN, Thio M, et al. The risk for hyperoxaemia after apnoea, bradycardia and hypoxaemia in preterm infants. Archives of disease in childhood Fetal and neonatal edition. 2014; 99:F269–73. [PubMed: 24668832]
14. Amy RW, Bowes D, Burri PH, Haines J, Thurlbeck WM. Postnatal growth of the mouse lung. J Anat. 1977; 124:131–51. [PubMed: 914698]
15. Hilgendorff A, Reiss I, Ehrhardt H, Eickelberg O, Alvira CM. Chronic lung disease in the preterm infant. Lessons learned from animal models. Am J Respir Cell Mol Biol. 2014; 50:233–45. [PubMed: 24024524]
16. Broytman O, Braun RK, Morgan BJ, et al. Effects of chronic intermittent hypoxia on allergen-induced airway inflammation in rats. Am J Respir Cell Mol Biol. 2015; 52:162–70. [PubMed: 25004109]
17. Peng YJ, Nanduri J, Yuan G, et al. NADPH oxidase is required for the sensory plasticity of the carotid body by chronic intermittent hypoxia. J Neurosci. 2009; 29:4903–10. [PubMed: 19369559]
18. Fabian RH, Perez-Polo JR, Kent TA. Extracellular superoxide concentration increases following cerebral hypoxia but does not affect cerebral blood flow. Int J Dev Neurosci. 2004; 22:225–30. [PubMed: 15245758]
19. Been JV, Lugtenberg MJ, Smets E, et al. Preterm birth and childhood wheezing disorders: a systematic review and meta-analysis. PLoS Med. 2014; 11:e1001596. [PubMed: 24492409]
20. Colin AA, McEvoy C, Castile RG. Respiratory morbidity and lung function in preterm infants of 32 to 36 weeks' gestational age. Pediatrics. 2010; 126:115–28. [PubMed: 20530073]
21. Kotecha SJ, Edwards MO, Watkins WJ, et al. Effect of preterm birth on later FEV1: a systematic review and meta-analysis. Thorax. 2013; 68:760–6. [PubMed: 23604458]
22. Jaakkola JJ, Ahmed P, Ieromnimon A, et al. Preterm delivery and asthma: a systematic review and meta-analysis. J Allergy Clin Immunol. 2006; 118:823–30. [PubMed: 17030233]
23. Hantos Z, Daroczy B, Suki B, Nagy S, Fredberg JJ. Input impedance and peripheral inhomogeneity of dog lungs. J Appl Physiol (1985). 1992; 72:168–78. [PubMed: 1537711]
24. O'Reilly M, Harding R, Sozo F. Altered small airways in aged mice following neonatal exposure to hyperoxic gas. Neonatology. 2014; 105:39–45. [PubMed: 24281398]
25. Wang H, Jafri A, Martin RJ, et al. Severity of neonatal hyperoxia determines structural and functional changes in developing mouse airway. Am J Physiol Lung Cell Mol Physiol. 2014; 307:L295–301. [PubMed: 24951774]
26. Stevens TP, Finer NN, Carlo WA, et al. Respiratory outcomes of the surfactant positive pressure and oximetry randomized trial (SUPPORT). J Pediatr. 2014; 165:240–9. e4. [PubMed: 24725582]
27. Elberson VD, Nielsen LC, Wang H, Kumar HS. Effects of intermittent hypoxia and hyperoxia on angiogenesis and lung development in newborn mice. J Neonatal Perinatal Med. 2016; 8:313–22.
28. Chang M, Bany-Mohammed F, Kenney MC, Beharry KD. Effects of a superoxide dismutase mimetic on biomarkers of lung angiogenesis and alveolarization during hyperoxia with intermittent hypoxia. Am J Transl Res. 2013; 5:594–607. [PubMed: 24093057]
29. Bedard K, Krause KH. The NOX family of ROS-generating NADPH oxidases: physiology and pathophysiology. Physiol Rev. 2007; 87:245–313. [PubMed: 17237347]

Author Manuscript Author Manuscript Author Manuscript Author Manuscript

30. Reyburn B, Di Fiore JM, Raffay T, et al. The Effect of Continuous Positive Airway Pressure in a Mouse Model of Hyperoxic Neonatal Lung Injury. Neonatology. 2016; 109:6–13. [PubMed: 26394387]

31. Shalaby KH, Gold LG, Schuessler TF, Martin JG, Robichaud A. Combined forced oscillation and forced expiration measurements in mice for the assessment of airway hyperresponsiveness. Respir Res. 2010; 11:82. [PubMed: 20565957]

32. Emery JL, Mithal A. The number of alveoli in the terminal respiratory unit of man during late intrauterine life and childhood. Arch Dis Child. 1960; 35:544–7. [PubMed: 13726619]

33. O'Reilly M, Hansbro PM, Horvat JC, Beckett EL, Harding R, Sozo F. Bronchiolar remodeling in adult mice following neonatal exposure to hyperoxia: relation to growth. Anat Rec (Hoboken). 2014; 297:758–69. [PubMed: 24443274]

Author Manuscript Author Manuscript Author Manuscript Author Manuscript

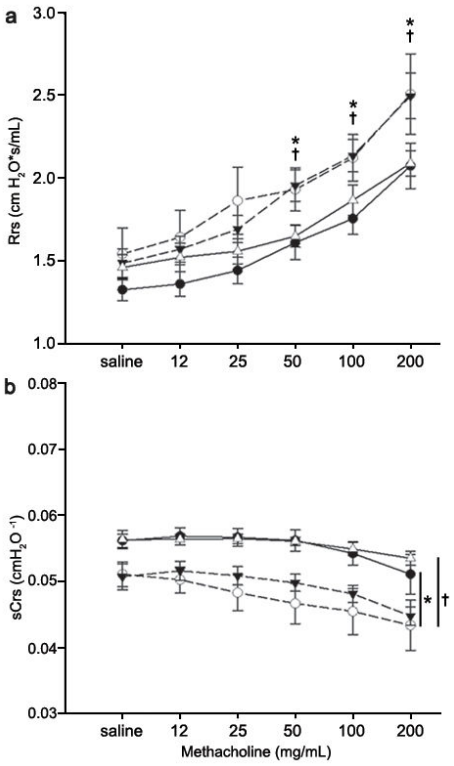

Figure 1.

Respiratory System Resistance (Rrs) and Specific Respiratory System Compliance (sCrs) and responses to methacholine in mechanically ventilated mice at P21. (a) Significant increases in Rrs were observed at higher methacholine doses of both groups who received intermittent hyperoxia ($CIH_{O/E}$, dashed line closed triangles and CIH_E, dashed line open circles) compared to room air controls (N_X, solid line closed circles). (b) Significant decrease in specific respiratory system compliance in $CIH_{O/E}$ and CIH_E at all doses compared to room air controls. No changes were observed between CIH_O (solid line, open triangles) and Nx. N=7-11 per group. $p < 0.05$: * $CIH_{O/E}$ vs N_X, †CIH_E vs N_X.

Author Manuscript Author Manuscript Author Manuscript Author Manuscript

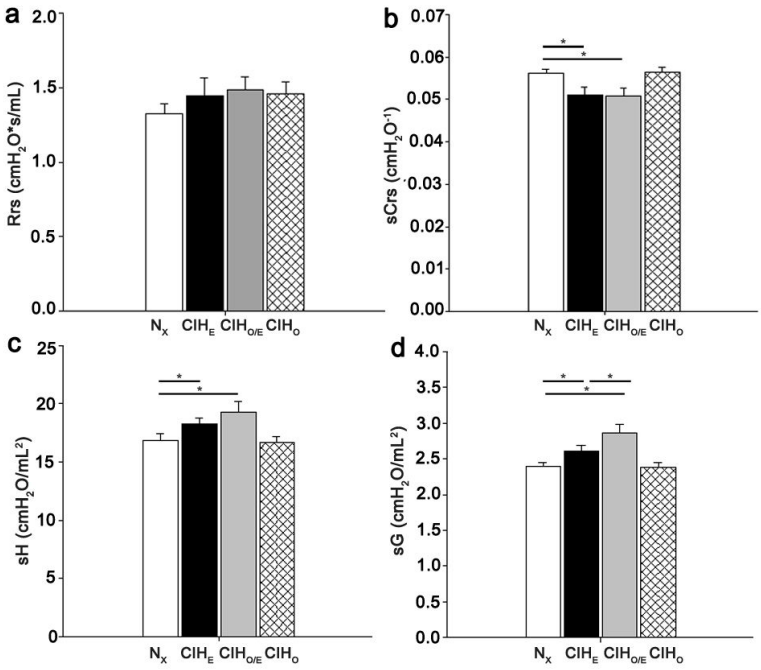

Figure 2.

Baseline Respiratory Mechanics at P21. (a) Respiratory System Resistance (Rrs) (b) Specific Respiratory System Compliance (sCrs) (c) Specific Elastance (sH). (d) Specific Tissue Damping (sG). N=7-11 per group. * $p < 0.05$

Author Manuscript Author Manuscript Author Manuscript Author Manuscript

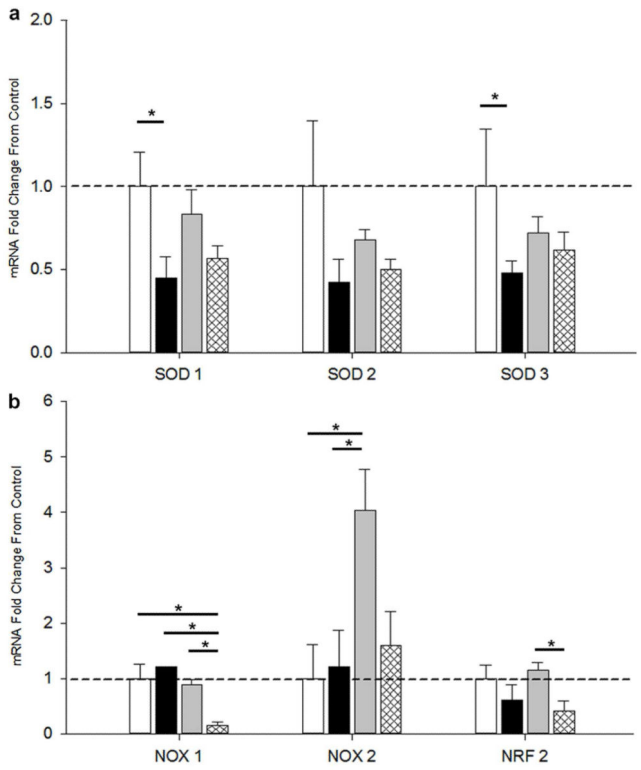

Figure 3.

Real-Time PCR of Lung Homogenates. RNA was extracted from whole lung homogenates of pups at P21. Fold-change of mRNA expression are demonstrated for groups CIH_E (second from left, black), $CIH_{O/E}$ (third from left, gray) and CIH_O (right, hatched) normalized to Nx (left, white) mice. (a) Antioxidant markers SOD1, SOD2, and SOD3 (b) Prooxidant makers of NOX1, NOX2, and NRF2. N=7-16 per group. *$p < 0.05$.

Author Manuscript Author Manuscript Author Manuscript Author Manuscript

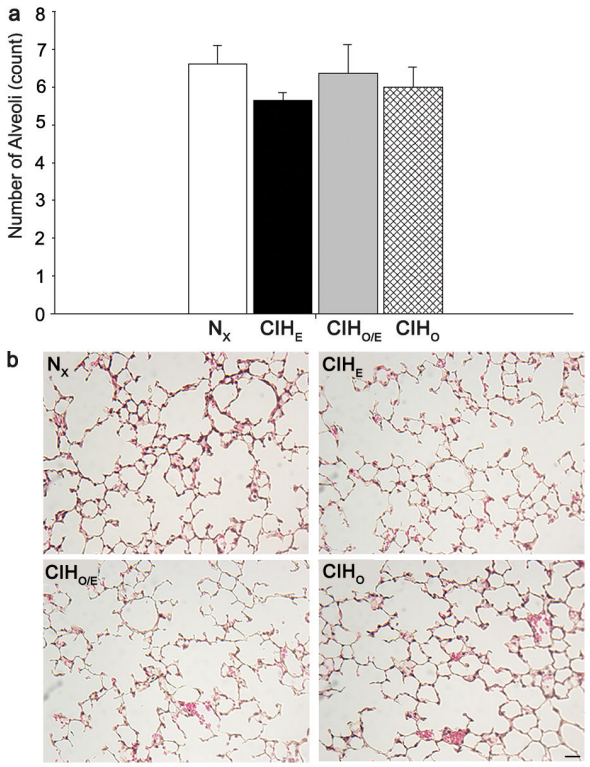

Figure 4.

Radial Alveolar Counts for all groups at P21. (a) Graph of counts for all four groups (b) Representative images of each group. No differences were seen between groups. Magnification bar 50μm. N=7-12 per group.

Author Manuscript Author Manuscript Author Manuscript Author Manuscript

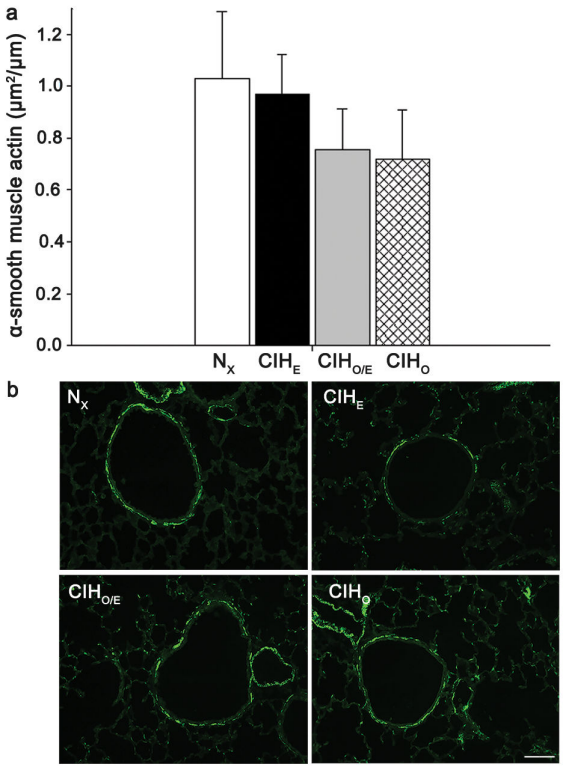

Figure 5.

Alpha-Actin in airway smooth muscle at P21. (a) Graph of smooth muscle alpha-actin expression in all four groups (b) Representative images from each group. No significant differences were observed between groups. Magnification bar 50μm. N=8-10 per group.

Author Manuscript Author Manuscript Author Manuscript Author Manuscript

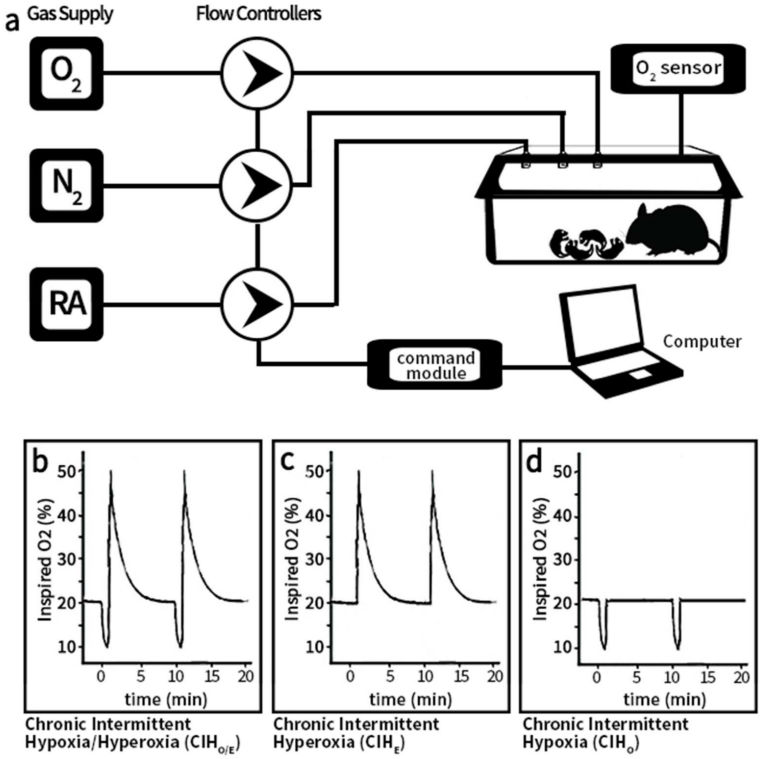

Figure 6.

(a) Schematic of Experimental Setup. Independent gas inputs of Nitrogen (N_2), Oxygen (O_2) and Room Air (RA) pass through computer-programmed flow controllers each connected to a command module and operated by a computer. Gas inputs feed into the animal cage attached to oximeter. Oxygen exposure paradigm for each experimental group with continuously monitored levels: (b) Chronic Intermittent Hypoxia/Hyperoxia (c) Chronic Intermittent Hyperoxia (d) Chronic Intermittent Hypoxia. Room air controls not illustrated. Two ten-minute repeating cycles illustrated. Cycles repeat 24hrs/day.